Published in final edited form as:
Circ Res. 2013 March 15; 112(6): 911–923. doi:10.1161/CIRCRESAHA.111.300179.

De-SUMOylation Enzyme of Sentrin/SUMO-Specific Protease 2 (SENP2) Regulates Disturbed Flow-Induced SUMOylation of ERK5 and p53 that Leads to Endothelial Dysfunction and Atherosclerosis

Kyung-Sun Heo[1], **Eugene Chang**[1], **Nhat-Tu Le**[1], **Hannah Cushman**[1], **Edward T.H. Yeh**[2], **Keigi Fujiwara**[1], and **Jun-ichi Abe**[1]

[1]Aab Cardiovascular Research Institute and Department of Medicine, University of Rochester School of Medicine and Dentistry, Rochester, New York, USA

[2]Department of Cardiology, University of Texas MD Anderson Cancer Center; Texas Heart Institute, St. Luke's Episcopal Hospital, Houston, TX 77030, USA

Abstract

Rationale—Disturbed flow induces pro-inflammatory and apoptotic responses in endothelial cells (ECs), causing them to become dysfunctional and subsequently pro-atherogenic.

Objective—Although a possible link between SUMOylation of p53 and ERK5 detected during endothelial apoptosis and inflammation has been suggested, the mechanistic insights, especially under the pro-atherogenic flow condition, remain largely unknown.

Methods and Results—SUMOylation of p53 and ERK5 was induced by disturbed flow but not by steady laminar flow. To examine the role of the disturbed flow-induced p53 and ERK5 SUMOylation, we utilized de-SUMOylation enzyme of sentrin/SUMO-specific protease 2 deficiency (*Senp2*$^{+/-}$) mice and observed a significant increase in endothelial apoptosis and adhesion molecule expression both in vitro and in vivo. These increases, however, were significantly inhibited in ECs overexpressing p53 and ERK5 SUMOylation site mutants. *Senp2*$^{+/-}$ mice exhibited increased leukocyte rolling along the endothelium, and accelerated formation of atherosclerotic lesions was observed in *Senp2*$^{+/-}$/*Ldlr*$^{-/-}$, but not *Senp2*$^{+/+}$/*Ldlr*$^{-/-}$, mice fed a high cholesterol diet. Notably, the extent of lesion size in the aortic arch of *Senp2*$^{+/-}$/*Ldlr*$^{-/-}$ mice was much larger than that in the descending aorta, also suggesting a crucial role of the disturbed flow-induced SUMOylation of proteins including p53 and ERK5 in atherosclerosis formation.

Conclusions—These data show the unique role of SENP2 on endothelial function under disturbed flow and suggest that SUMOylation of p53 and ERK5 by disturbed flow contributes to the atherosclerotic plaque formation. Molecules involved in this newly discovered signaling will be useful targets for controlling ECs dysfunction and consequently atherosclerosis formation.

Address correspondence to: Dr. Jun-ichi Abe, Aab Cardiovascular Research Institute and Department of Medicine, University of Rochester School of Medicine and Dentistry, 601 Elmwood Ave, Box CVRI, Rochester, NY 14642, Tel: (585) 276-9794, Fax: (585) 276-9830, Jun-ichi_Abe@urmc.rochester.edu.
K-S.H. and E.C. contributed equally to this study.

DISCLOSURES
None.

Keywords

Atherosclerosis; disturbed flow; endothelial cells; SENP2; SUMOylation; shear stress; signal transduction

INTRODUCTION

Atherosclerosis is a focalized disease that develops preferentially in areas within large arteries that are exposed to disturbed blood flow patterns[1, 2]. Endothelial cells (ECs) form the first line of defense against atherosclerotic development by releasing vasodilators and anti-inflammatory molecules. Many of the anti-atherosclerotic signals are activated by steady laminar flow, which down-regulates a number of inflammatory genes in ECs as documented by numerous transcriptional profiling studies[3]. However, in certain regions of the arterial tree, such as vessel curvatures, branches and bifurcations, disturbed flow develops and activates the pro-inflammatory and pro-apoptotic genes in ECs, which leads to their dysfunction[4]. This endothelial dysfunction caused by disturbed flow is thought to be one of the primary culprits in the progression of atherosclerosis[5]. However, signal transduction pathways activated by disturbed flow in ECs to cause endothelial dysfunction and subsequent atherosclerosis remain poorly understood.

Protein modifications such as phosphorylation, SUMOylation, and ubiquitination have come into focus as important regulators of signaling due to the transient nature of these modifications and they can reversibly alter physiological states of cells. Particularly interesting is SUMOylation, a unique post-translational modification akin to ubiquitination, that conjugates small ubiquitin-like proteins called SUMO (Small Ubiquitin-like MOdifier) to target proteins and affects a number of processes including the localization, degradation, binding, and activity of SUMOylated proteins[6]. Sentrin/SUMO-specific protease 2 (SENP2) is a de-SUMOylation enzyme that is important for both processing new SUMO proteins for conjugation as well as deconjugating SUMO from SUMOylated proteins[7–9]. Although six isoforms of SENPs exist in humans (SENP1–3 and 5–7), SENP2 specifically regulates p53 through Mdm2 de-SUMOylation, leading to apoptosis of cells[10, 11].

In ECs, we have found that SUMOylation plays an important role in regulating actin filament remodeling[12], migration[12], inflammation[13], and apoptosis[5] that occur in response to flow stimulation. We have recently reported that disturbed flow activates protein kinase Cζ (PKCζ) to induce p53 SUMOylation and subsequently increases endothelial apoptosis[5]. We have also reported that SUMOylation of extracellular signal-regulated kinase-5 (ERK5) inhibits ERK5-dependent activation of the anti-inflammatory molecule Krüppel-like factor 2 (KLF2), resulting in the loss of anti-inflammatory property of ERK5 that is normally activated by laminar shear stress[13]. Thus, it appears that SUMOylation of p53 and ERK5 plays a role in mediating endothelial inflammation and apoptosis. However, the role of SUMOylation, especially SENP2, in endothelial dysfunction and subsequent atherosclerosis remains unclear. We hypothesize that SENP2 regulates SUMOylation levels of p53 and ERK5 and may determine the healthy or diseased state of ECs, especially under the disturbed flow condition.

METHODS

Detailed descriptions of the Materials and Methods are available in the Online Data Supplement. A brief description of the methods used is given below.

Isolation of mouse aortic ECs (MAECs) and lung ECs (MLECs)

Methods for isolation of MAECs[14] or MLECs[15] were modified from published protocols.

ERK5 transcriptional activity analysis

ERK5 transcriptional activity was assayed by the dual-luciferase reporter assay[16].

Immunoprecipitation (SUMO assay) and Western blot analysis

Immunoprecipitation and Western blotting analysis was performed as described previously[17].

Real-time PCR assay

Total RNA was extracted using the TRIzol reagent according to the manufacturer's instructions and reverse transcriptase reactions (PCR) were performed as described previously[18].

Analysis of apoptosis

Apoptosis was quantified by both TUNEL staining and active caspase-3 expression, as described previously[7].

Mice

All animal procedures were performed with the approval from the University Committee on Animal Resources at the University of Rochester. Non-transgenic littermate control mice (*Senp2*$^{+/+}$, n=12) and SENP2 deficiency mice (*Senp2*$^{+/-}$, n=12) or *Senp2*$^{+/+}$/*Ldlr*$^{-/-}$ (n=25) and *Senp2*$^{+/-}$/*Ldlr*$^{-/-}$ (n=25) (all female) in the C57BL/6J background were used.

En Face immunostaining

The steady laminar flow and disturbed flow areas within the aorta were identified, and immunostaining was performed as described previously[5].

Leukocyte rolling assay and vessel diameter measurements

Intravital microscopy was performed as previously described[19]. Briefly, the mesentery was externalized, and then rolling of rhodamine 6G labeled leukocytes in arterioles (≈ 20 μm in diameter) was recorded with a digital video camera.

Bone marrow transplantation (BMT)

BMT was performed as previously reported with minor modifications[20]. Briefly, female *Ldlr*$^{-/-}$ recipient mice at 6 weeks of age received a single semi-lethal dose of 900 rad irradiation using an RS2000 irradiator (Rad Source Technologies, Suwanee, GA). BM cells were harvested from *Senp2*$^{+/+}$ or *Senp2*$^{+/-}$ non-irradiated donor mice and 6 x 10^6 cells were injected via the postorbital vein into recipient mice immediately after irradiation.

Statistical analysis

Data are presented as mean ± S.D. Statistical analyses by Wilcoxon signed-rank test, Kruskal-Wallis test, and Bonferroni multiple-comparison test were performed using the GraphPad Prism program, version 4.00 (GraphPad Software, Inc., CA) as described previously[21].

RESULTS

SENP2 inhibits endothelial apoptosis by down-regulating p53 SUMOylation

SUMOylation is a tightly regulated process within the cell and proteins constantly undergo SUMOylation and de-SUMOylation, and SENPs are the enzymes primarily responsible for deconjugating SUMOylated proteins. It has recently been reported that cytosolic p53 directly interacts with Bcl-2 and loses its anti-apoptotic stabilization effect on the outer mitochondrial membrane[22, 23]. We have also reported the crucial role of p53 SUMOylation on the interaction of Bcl-2 and p53 and subsequent disturbed flow-induced apoptosis in ECs[7]. Therefore, in this study we first investigated the role of SENP2 in endothelial apoptosis by transfecting human aortic endothelial cells (HAECs) or human umbilical vein endothelial cells (HUVECs) with human SENP2 siRNA, stimulating them with disturbed flow, and then staining them with the TUNEL reagent. A knockdown of SENP2 enhanced endothelial apoptosis under both static and disturbed flow conditions (Figs. 1A and Online Fig. I). Increased apoptosis in SENP depleted HAECs under both static and disturbed flow conditions were also detected by the expression of cleaved-caspase3 (Fig. 1B). Next, we investigated the mechanism for this apoptosis by checking the role of SENP2 in regulating p53 SUMOylation. As suspected, knockdown of SENP2 increased p53 SUMOylation in HAECs (Fig. 1C), mouse aortic endothelial cells (MAECs, Online Fig. IIA), and HUVECs (Online Fig. IIB), while overexpression of adenoviral SENP2 (Ad-SENP2) ablated p53 SUMOylation (Fig. 1E). In contrast to ECs stimulated with disturbed flow, those stimulated with steady laminar flow showed a decrease in p53 SUMOylation compared to those kept under the static condition (Fig. 1D). Furthermore, in agreement with our previous report[7], which showed the importance of p53 SUMOylation state on the interaction between Bcl-2 and p53, depletion of SENP2 increased Bcl-2-p53 interaction (Fig. 1F).

To determine the involvement of p53 SUMOylation in the reduction of SENP2-mediated endothelial apoptosis, we isolated mouse lung endothelial cells (MLECs) from the heterozygous *Senp2*$^{+/-}$ and littermate wild type *Senp2*$^{+/+}$ mice and determined constitutive levels of p53 SUMOylation. We found significantly increased p53 SUMOylation in the MLECs from *Senp2*$^{+/-}$ mice compared with those from *Senp2*$^{+/+}$ (Fig. 2A). p53 SUMOylation was also increased in MAECs isolated from *Senp2*$^{+/-}$ mice compared with those isolated from control *Senp2*$^{+/+}$ mice (Fig. 2B, 1st vs 3rd lane). However, the enhancement of p53 SUMOylation induced by disturbed flow in *Senp*$^{+/-}$ MAECs compared with control *Senp*$^{+/+}$ cells was marginal (Fig. 2B, 2nd vs 4th lane). The reason for this is not clear, but it is possible that p53 SUMOylation may be at the maximum level in MAECs isolated from *Senp2*$^{+/-}$ mice so that disturbed flow cannot further augment the p53 SUMOylation level in these cells. However, when we examined the p53 and ERK5 SUMOylation in HAECs (Figs. 1C and 3C), mouse aortic endothelial cells (MAECs, Online Fig. IIA), and HUVECs (Online Figs. IIB and C) using a siRNA of SENP2 in vitro, we found synergic effect of disturbed flow on the p53/ERK5 SUMOylation by SENP2 depletion. Since the disturbed flow decreased de-SUMOylation activity of SENP2 against p53 and ERK5, the depletion of SENP2 study itself has its own limitation to prove the role of SENP2 on p53 and ERK5 SUMOylation under d-flow.

Next, we determine the effect of p53 SUMOylation on EC apoptosis using adenoviruses containing wild type p53 (Ad-p53-WT) and the SUMOylation site mutant p53-K386R (Ad-p53-K386R). A significant increase in apoptosis was noted in ECs from *Senp2*$^{+/-}$ mice compared with those from *Senp2*$^{+/+}$ transduced by Ad-LacZ control, confirming the data obtained using HUVECs (Fig. 2C). Increased apoptosis in *Senp2*$^{+/-}$ MLECs was also detected by the expression of cleaved-caspase3 (Fig. 4F). We then transduced Ad-p53-WT or Ad-p53-K368R mutant in MLECs isolated from *Senp2*$^{+/-}$ and found that the p53

SUMOylation mutant significantly inhibited apoptosis (Fig. 2C), demonstrating the importance of SENP2 in regulating p53 SUMOylation-mediated ECs apoptosis.

SENP2 inhibits disturbed flow-mediated endothelial ERK5 SUMOylation

Previously, we have reported that reactive oxygen species (ROS) or advanced glycation end products induce ERK5 SUMOylation, inhibiting its transactivation function and subsequently decreasing expression of KLF2 and eNOS[13]. However, it is not known if disturbed flow regulates ERK5 SUMOylation or if it is involved in EC inflammation. First, we examined whether disturbed flow could increase ERK5 SUMOylation and found that it significantly heightened ERK5 SUMOylation (Fig. 3A). In contrast, steady laminar flow down-regulated ERK5 SUMOylation[24] (Fig. 3B). Second, to investigate the involvement of endogenous SENP2 on disturbed flow-induced ERK5 SUMOylation, we depleted SENP2 expression by siRNA in both HAECs and HUVECs and found that SENP2 depletion increased the baseline level of ERK5 SUMOylation (3rd lane) and disturbed flow-induced ERK5 SUMOylation was significantly amplified (4th lane) in both cell types (Figs. 3C and Online Fig. IIC). We also performed a gain-of-function study and found that overexpression of SENP2 completely abolished the disturbed flow effect on ERK5 SUMOylation (Fig. 3D), suggesting a critical role of SENP2 in disturbed flow-induced ERK5 SUMOylation.

ERK5 transactivation and expression of eNOS and KLF2 are inhibited while adhesion molecule expression is increased by disturbed flow in a SENP2-dependent manner

Since ERK5 SUMOylation by disturbed flow decreased ERK5 transcriptional activity and consequent expression of KLF2 and eNOS[13], we first determined the effects of depletion and overexpression of SENP2 on ERK5 transcriptional activity. Disturbed flow decreased ERK5 transcriptional activity, which was further decreased by SENP2 siRNA, whereas Ad-SENP2 transduction reversed it (Fig. 3E). Next, we investigated the KLF2 and eNOS expression and found that their expression was decreased by disturbed flow (Fig. 3F). SENP2 deficiency inhibited their expression under the static condition, but it did so more strongly under the disturbed flow condition (Fig. 3F). In contrast, when SENP2 was overexpressed, the expression of KLF2 and eNOS increased and the disturbed flow effect was abolished (Fig. 3G).

KLF2 antagonizes inflammatory gene expression[13]. Therefore, we also examined adhesion molecule expression induced by disturbed flow. Disturbed flow increased the expression of E-selectin, ICAM-1, and VCAM-1, which was significantly enhanced by the depletion of SENP2 (Fig. 3H), while its overexpression had the opposite effect (Fig. 3I). These data suggest a crucial role of SENP2 in regulating ECs inflammation.

Inhibition of KLF2 and eNOS and up-regulated adhesion molecule expression in MLECs from Senp2$^{+/-}$ mice

MLECs and MAECs were isolated from *Senp2*$^{+/-}$ and *Senp2*$^{+/+}$ mice, and ERK5 SUMOylation levels were examined. ERK5 SUMOylation was significantly higher in *Senp2*$^{+/-}$ MLECs compared with *Senp2*$^{+/+}$ MLECs (Fig. 4A). Of note, compared with HUVECs, MLECs and MAECs expressed a greater level of the lower molecular weight ERK5 isoform at around 75 kDa as we previously reported[25]. The same results were obtained in the *Senp2*$^{+/-}$ vs *Senp2*$^{+/+}$ MAEC comparison (Fig. 4B). However, the enhancement of ERK5 SUMOylation by disturbed flow in *Senp*$^{+/-}$ cells was also marginal as we have shown in p53 SUMOylation in Fig. 2B. ERK5 transcriptional activity and the KLF2 and eNOS mRNA expression were decreased in *Senp2*$^{+/-}$ MLECs (Figs. 4C and D).

Since KLF2 has an anti-inflammatory effect in ECs[26, 27], we examined the role of SENP2 in cytokine-mediated EC inflammation. Increased expression of ICAM-1 and VCAM-1

mRNAs was noted in *Senp2*$^{+/-}$MLECs compared with *Senp2*$^{+/+}$ MLECs (Fig. 4E). The expression of E-selectin, ICAM-1, and VCAM-1 mRNAs was induced by TNFα stimulation in *Senp2*$^{+/+}$ MLECs, which was further increased in *Senp2*$^{+/-}$MLECs. We also found increased expression of E-selectin, ICAM-1, and VCAM-1 proteins in *Senp2*$^{+/-}$ MLECs (Fig. 4F). It is possible that increased ERK5 SUMOylation under the inflammatory condition is due to reduced SENP2 expression in ECs.

ERK5 SUMOylation inhibits KLF2 and eNOS and up-regulates adhesion molecule expression in Senp2$^{+/-}$ECs

To determine the effects of ERK5 SUMOylation on SENP2-mediated anti-inflammatory events in ECs, we transduced adenoviruses containing ERK5 wild type (Ad-ERK5-WT) and ERK5 SUMOylation site mutant (Ad-ERK5-K6/22R) in *Senp2*$^{+/-}$ cells. Increased expression of E-selectin, VCAM-1, and ICAM-1 mRNA in *Senp2*$^{+/-}$ MLECs was partially down-regulated in cells transduced by Ad-ERK5-WT, but their expression was completely inhibited in *Senp2*$^{+/-}$ MLECs transduced by the Ad-ERK5-K6/22R mutant (Fig. 5A). Furthermore, reduced expression of eNOS and KLF2 mRNAs in *Senp2*$^{+/-}$ MLECs was blunted by Ad-ERK5-WT, but Ad-ERK5-K6/22R mutant transduction strongly up-regulated their mRNA levels (Fig. 5B). We confirmed similar expression levels of ERK5-WT and ERK5-K6/22R mutant in MLECs (Fig. 5C). E-selectin, VCAM-1, and ICAM-1 protein expression levels were significantly decreased in *Senp2*$^{+/-}$ MLECs transduced by Ad-ERK5-K6/22R mutant compared with those in Ad-LacZ or Ad-ERK5-WT transduced *Senp2*$^{+/-}$ MLECs (Fig. 5D). These data suggest a crucial role of ERK5 SUMOylation in the SENP2-mediated down-regulation of EC inflammation.

To determine the role of ERK5 SUMOylation in apoptosis induced by disturbed flow, we transduced Ad-ERK5-WT and Ad-ERK5-K6/22R in MAECs from *Senp2*$^{+/+}$ mice. Both Ad-ERK5-WT and Ad-ERK5-K6/22R reduced the disturbed flow-induced terminal deoxy-ribonucleotide transferase (TdT)-mediated dUTP nick-end labeling (TUNEL) staining and cleaved-caspase3 expression (Figs. 5E–G), suggesting that ERK5 indeed inhibits apoptosis as we have previously reported[28] but that ERK5 SUMOylation is not involved in this process. Since we have reported that SUMOylation does not affect ERK5 kinase activity[24], we assume that another ERK5 kinase substrate such as SGK[29] may be involved in this process.

En face immunohistochemistry for apoptosis, E-selectin, and VCAM-1 in the aorta of Senp2$^{+/+}$ and Senp2$^{+/-}$ mouse

We investigated whether reduced SENP2 expression affected EC apoptosis *in vivo*. En face preparations of aortas of 7-week-old *Senp2*$^{+/+}$ mice were co-immunostained for TUNEL and VE-cadherin (VE-cad; red) (Fig. 6A) or AnnexinV (red) and VE-cad (green) (Fig. 6B). For imaging, we focused on areas exposed to either disturbed flow (lesser curvature of aortic arch) or steady laminar flow (greater curvature of aortic arch) as described previously[30] (see Methods). While the TUNEL and annexinV positive cells were rare in the steady laminar flow area, they were frequently detected in the disturbed flow area in *Senp2*$^{+/+}$ mice (Figs. 6A and B). Interestingly, we found increased numbers of TUNEL and annexinV positive cells in both disturbed and steady laminar flow areas in the *Senp2*$^{+/-}$ mice (Figs. 6A and B), confirming a critical role of SENP2 in disturbed flow-mediated apoptosis *in vivo*.

Since the increased expression of E-selectin and VCAM-1 in disturbed flow areas has been reported, we investigated their expression in the *Senp2*$^{+/+}$ and *Senp2*$^{+/-}$ mice (Figs. 6D and E). Staining by both antiE-selectin and anti-VCAM-1 was significantly stronger in disturbed flow areas than in steady laminar flow areas in *Senp2*$^{+/+}$ mice. We found that the expression of E-selectin and VCAM-1 was markedly increased in the steady laminar flow area of

Senp2$^{+/-}$ mice compared with *Senp2*$^{+/+}$ mice (Figs. 6D–F). Non-immune control IgG yielded no visual fluorescence in both disturbed and steady laminar flow areas (Online Fig. III). These data suggest a critical role of SENP2 in regulating the endothelial E-selectin and VCAM-1 expression *in vivo*.

ECs dysfunction in Senp2$^{+/-}$ mice

We investigated leukocyte rolling in and acetylcholine (ACh)-induced dilation of mesenteric arterioles of *Senp2*$^{+/-}$ and *Senp2*$^{+/+}$ mice. Increased leukocyte rolling was observed in *Senp2*$^{+/-}$ compared with *Senp2*$^{+/+}$ mice (Figs. 7A–C and Online Movies I–II). No differences were found in vessel diameter or shear rate between these animals (data not shown). ACh-induced arteriole dilatation was decreased in *Senp2*$^{+/-}$ mice (Fig. 7C, left panel). However, EC-independent vasodilation by sodium nitroprusside (SNP) was indistinguishable between the two mice (Fig. 7C, right panel). We also investigated effects of L-NG-Nitroarginine Methyl Ester (L-NAME) in both *Senp2*$^{+/+}$ and *Senp2*$^{+/-}$ mice on vessel responses to ACh and found that L-NAME pretreatment abolished vasodilatation by ACh, but not SNP, in both *Senp2*$^{+/-}$ and *Senp2*$^{+/+}$ mice, suggesting that ACh-mediated vasodilatation was due to NO production (Fig. 7D).

Reduced SENP2 expression elevates atherosclerotic plaque formation, which is mediated by vascular but not by hematopoietic cells

To examine the role of SENP2 in atherosclerosis formation, we generated a double-knock out *Senp2*$^{+/-}$/*Ldlr*$^{-/-}$ mouse model and compared the extent of atherosclerosis formation in these mice with that in *Senp2*$^{+/+}$/*Ldlr*$^{-/-}$ mice after 16-week on a high cholesterol diet. The lesion area in both aortic arch and descending aorta was significantly larger in *Senp2*$^{+/-}$/*Ldlr*$^{-/-}$ than *Senp2*$^{+/+}$/*Ldlr*$^{-/-}$ mice (Fig. 8A, upper two panels). We also found that the lesion size observed in histological sections of the aortic valve region was larger in *Senp2*$^{+/-}$/*Ldlr*$^{-/-}$ than *Senp2*$^{+/+}$/*Ldlr*$^{-/-}$ mice (Fig. 8A, lower two panels). Interestingly, the extent of increase in the lesion size in the aortic arch of *Senp2*$^{+/-}$/*Ldlr*$^{-/-}$ mice was much larger than that in descending aorta (Fig. 8A, upper two panels). It is well known that the lesser curvature area of the aortic arch is subjected to disturbed flow[31]. Therefore, the significant lesion size expansion in this area in *Senp2*$^{+/-}$/*Ldlr*$^{-/-}$ mice suggests the crucial role of disturbed flow-induced SUMOylation of proteins including p53 and ERK5 on atherosclerosis formation. No differences were noted in their body weight and blood contents of total cholesterol, LDL cholesterol and HDL cholesterol (Online Fig. IV). To investigate whether the increased atherosclerotic formation in *Senp2*$^{+/-}$/*Ldlr*$^{-/-}$ mice was due to SENP2 reduction in vessel cells (ECs) or hematopoietic cells, we performed bone marrow transplantation. Bone marrow cells from *Senp2*$^{+/+}$ or *Senp2*$^{+/-}$ mice were transplanted into 6-week-old semi-lethally irradiated *Ldlr*$^{-/-}$ mice. After 6 weeks of recovery, the mice were given a high cholesterol diet for 12 additional weeks (Fig. 8B). Successful chimerism of bone marrow cells was confirmed by Western blotting against total lysates of blood cells isolated from recipient mice (Fig. 8C, right lower panel). *Ldlr*$^{-/-}$ mice that received *Senp2*$^{+/-}$ hematopoietic cells showed the same extent of vascular lesion development in the aortic root as the mice given cells from *Senp2*$^{+/+}$ donors (Fig. 8C), suggesting that vascular SENP2 expression regulates atherosclerosis formation.

DISCUSSION

Disturbed flow induces a pro-inflammatory state in ECs that counters the beneficial effects of laminar shear stress[4]. The loss of this protective signaling makes the endothelium vulnerable to becoming dysfunctional and subsequently to developing atherosclerosis. Post-translational modifications of proteins have emerged as important regulators of signaling due to the vast array of reversible changes they can induce in both physiological and

pathological pathways. SUMOylation is one of the most dynamic post-translational modifications with its diverse repertoire of effects ranging from protein localization to transcriptional regulation and DNA binding[6, 32]. In this study we found that disturbed flow induced SUMOylation of p53 and ERK5, leading to ECs apoptosis and inflammation, respectively (Fig. 8D). We found that reduced expression of SENP2 increased both p53 and ERK5 SUMOylation, hence increased EC dysfunction and inflammation, and accelerated atherosclerosis formation *in vivo*. We also found that in mice, 1) reduced expression of SENP2 in hematopoietic cells did not affect atherosclerosis formation, 2) ACh- but not SNP-induced vasodilation was dampened by reduced SENP2, and 3) reduced SENP2 levels increased apoptosis and E-selectin and VCAM-1 expression *in vivo*. These results indicate for the first time that SENP2 function plays an important role in atherosclerosis formation, at least in mice. We caution here that ERK5 and p53 are most likely not the only proteins whose SUMOylation levels are increased by SENP2 depletion, and it is possible that other SUMOylatable molecules may be involved in the increased vascular events in *Senp2*$^{+/-}$/*Ldlr*$^{-/-}$ mice. However, since the disturbed flow-induced adhesion molecule expression and EC apoptosis were inhibited by a p53 or ERK5 SUMOylation mutant, we may tentatively conclude that SUMOylation of p53 and ERK5 has significant effects on disturbed flow-induced endothelial apoptosis and inflammation, respectively (Fig. 8D).

To our knowledge this is the first report that describes an important role of SENP2 in disturbed flow-induced EC dysfunction and inflammation. Since we did not find a decrease in SENP2 expression under the disturbed flow condition, it is possible that disturbed flow inhibits its activity or changes its cellular localization, which may involve some post-translational modifications. In fact, it has been reported that SENP2 contains both a bipartite nuclear localization signal (NLS) and a CRM1-dependent nuclear export signal (NES) and that its function can be regulated by nucleo-cytoplasmic shuttling[33]. Due partly to the lack of appropriate antibodies for immunostaining, SENP2 cellular localization was not studied at this time. We will focus on this issue in our next study.

In this study, we have reported the involvement of SENP2 on endothelial inflammation. It was reported that in mouse embryonic fibroblasts (MEFs), SENP2 efficiently associated with NEMO (NF-κB essential modulator), de-SUMOylated NEMO, inhibited NF-κB activation, and accelerated cell death induced by DNA damage[34]. However, *Senp2*$^{-/-}$ MEFs were not resistant to cell death induced by TNFα (+ cyclohexomide)[34]. In our current study, we found that TNFα induced a significant increase in adhesion molecule expression in *Senp2*$^{+/-}$ ECs. Thus, the regulatory mechanism of SENP2 on TNFα-mediated signaling might be different between ECs and MEFs. It is possible that NEMO SUMOylation in *Senp2*$^{+/-}$ECs is also involved in EC inflammation, but we found that the ERK5 SUMOylation mutant significantly inhibited adhesion molecule induction in *Senp2*$^{+/-}$ ECs. This suggests a crucial role of ERK5 SUMOylation in regulating EC inflammation. The possible interplay between NEMO and ERK5 on regulating NF-κB signaling needs to be studied further.

An expanded Results and Discussion section is available in the Online Data Supplement.

Supplementary Material

Refer to Web version on PubMed Central for supplementary material.

Acknowledgments

We thank Craig Morrell for the support of intravital microscopy, Alison Hobbins for kindly providing HUVECs, and Cheryl Hurley and Sara Hillman for technical assistance. Edward T.H. Yeh is the McNair Scholar of the Texas Heart Institute.

SOURCES OF FUNDING

This work is supported by grants from the National Institute of Health (NIH) to Dr. Abe (HL-108551, HL-064839, and HL-102746) and from the American Heart Association (AHA) to Drs. Fujiwara (11GRNT5850001) and Heo (12SDG11690003).

Nonstandard Abbreviations

ACh	Acetylcholine
Ad	Adenovirus
Ad-ERK5-K6/22R	Adenovirus containing ERK5 SUMOylation site mutant
Ad-ERK5-WT	Adenovirus containing ERK5 wild type
ECs	Endothelial cells
eNOS	Endothelial nitiric oxide synthase
HAECs	Human arotic endothelial cells
HUVECs	Human umbilical vein endothelial cells
KLF-2	Krüppel-like factor 2
L-NAME	L-NG-Nitroarginine Methyl Ester
MAECs	Mouse aortic endothelial cells
MLECs	Mouse lung endothelial cells
MEFs	Mouse embryonic fibroblasts
NEMO	NF-kB essential modulator
NES	Nuclear export signal
NLS	Nuclear localization signal
PKCζ	Protein kinase Cζ
SENP2	Sentrin/SUMO-specific protease 2
SNP	Nitroprusside
SUMO	Small Ubiquitin-like MOdifier
TUNEL	Terminal deoxy-ribonucleotide transferase (TdT)-mediated dUTP nick-end labeling (TUNEL)

References

1. Libby P, Ridker PM, Maseri A. Inflammation and atherosclerosis. Circulation. 2002; 105:1135–1143. [PubMed: 11877368]
2. Lusis AJ. Atherosclerosis. Nature. 2000; 407:233–241. [PubMed: 11001066]
3. Berk BC. Atheroprotective signaling mechanisms activated by steady laminar flow in endothelial cells. Circulation. 2008; 117:1082–1089. [PubMed: 18299513]
4. Malek AM, Alper SL, Izumo S. Hemodynamic shear stress and its role in atherosclerosis. JAMA : the journal of the American Medical Association. 1999; 282:2035–2042. [PubMed: 10591386]
5. Heo KS, Lee H, Nigro P, Thomas T, Le NT, Chang E, McClain C, Reinhart-King CA, King MR, Berk BC, Fujiwara K, Woo CH, Abe J. Pkczeta mediates disturbed flow-induced endothelial apoptosis via p53 sumoylation. J Cell Biol. 2011; 193:867–884. [PubMed: 21624955]
6. Geiss-Friedlander R, Melchior F. Concepts in sumoylation: A decade on. Nat Rev Mol Cell Biol. 2007; 8:947–956. [PubMed: 18000527]

7. Witty J, Aguilar-Martinez E, Sharrocks AD. Senp1 participates in the dynamic regulation of elk-1 sumoylation. Biochem J. 2010; 428:247–254. [PubMed: 20337593]
8. Yeh ET. Sumoylation and de-sumoylation: Wrestling with life's processes. J Biol Chem. 2009; 284:8223–8227. [PubMed: 19008217]
9. Cheng J, Wang D, Wang Z, Yeh ET. Senp1 enhances androgen receptor-dependent transcription through desumoylation of histone deacetylase 1. Mol Cell Biol. 2004; 24:6021–6028. [PubMed: 15199155]
10. Jiang M, Chiu SY, Hsu W. Sumo-specific protease 2 in mdm2-mediated regulation of p53. Cell Death Differ. 2011; 18:1005–1015. [PubMed: 21183956]
11. Chiu SY, Asai N, Costantini F, Hsu W. Sumo-specific protease 2 is essential for modulating p53-mdm2 in development of trophoblast stem cell niches and lineages. PLoS Biol. 2008; 6:e310. [PubMed: 19090619]
12. Chang E, Heo KS, Woo CH, Lee H, Le NT, Thomas TN, Fujiwara K, Abe J. Mk2 sumoylation regulates actin filament remodeling and subsequent migration in endothelial cells by inhibiting mk2 kinase and hsp27 phosphorylation. Blood. 2011; 117:2527–2537. [PubMed: 21131586]
13. Woo CH, Shishido T, McClain C, Lim JH, Li JD, Yang J, Yan C, Abe J. Extracellular signal-regulated kinase 5 sumoylation antagonizes shear stress-induced antiinflammatory response and endothelial nitric oxide synthase expression in endothelial cells. Circ Res. 2008; 102:538–545. [PubMed: 18218985]
14. Kobayashi M, Inoue K, Warabi E, Minami T, Kodama T. A simple method of isolating mouse aortic endothelial cells. J Atheroscler Thromb. 2005; 12:138–142. [PubMed: 16020913]
15. Lim YC, Luscinskas FW. Isolation and culture of murine heart and lung endothelial cells for in vitro model systems. Methods Mol Biol. 2006; 341:141–154. [PubMed: 16799196]
16. Akaike M, Che W, Marmarosh NL, Ohta S, Osawa M, Ding B, Berk BC, Yan C, Abe J. The hinge-helix 1 region of peroxisome proliferator-activated receptor gamma1 (ppargamma1) mediates interaction with extracellular signal-regulated kinase 5 and ppargamma1 transcriptional activation: Involvement in flow-induced ppargamma activation in endothelial cells. Mol Cell Biol. 2004; 24:8691–8704. [PubMed: 15367687]
17. Heo KS, Fujiwara K, Abe J. Disturbed-flow-mediated vascular reactive oxygen species induce endothelial dysfunction. Circ J. 2011; 75:2722–2730. [PubMed: 22076424]
18. Heo KS, Chang E, Takei Y, Le NT, Woo CH, Sullivan MA, Morrell C, Fujiwara K, Abe JI. Phosphorylation of protein inhibitor of activated stat1 (pias1) by mapk-activated protein kinase-2 (mk2) inhibits endothelial inflammation via increasing both pias1 transrepression and sumo e3 ligase activity. Arterioscler Thromb Vasc Biol. 2012
19. Cambien B, Bergmeier W, Saffaripour S, Mitchell HA, Wagner DD. Antithrombotic activity of tnf-alpha. J Clin Invest. 2003; 112:1589–1596. [PubMed: 14617760]
20. Gerloff J, Korshunov VA. Immune modulation of vascular resident cells by axl orchestrates carotid intima-media thickening. Am J Pathol. 2012; 180:2134–2143. [PubMed: 22538191]
21. Le NT, Heo KS, Takei Y, Lee H, Woo CH, Chang E, McClain C, Hurley C, Wang X, Li F, Xu H, Morrell C, Sullivan MA, Cohen MS, Serafimova IM, Taunton J, Fujiwara K, Abe JI. A crucial role for p90rsk-mediated reduction of erk5 transcriptional activity in endothelial dysfunction and atherosclerosis. Circulation. 2012
22. Mihara M, Erster S, Zaika A, Petrenko O, Chittenden T, Pancoska P, Moll UM. P53 has a direct apoptogenic role at the mitochondria. Mol Cell. 2003; 11:577–590. [PubMed: 12667443]
23. Bischof O, Schwamborn K, Martin N, Werner A, Sustmann C, Grosschedl R, Dejean A. The e3 sumo ligase piasy is a regulator of cellular senescence and apoptosis. Mol Cell. 2006; 22:783–794. [PubMed: 16793547]
24. Woo CH, Massett MP, Shishido T, Itoh S, Ding B, McClain C, Che W, Vulapalli SR, Yan C, Abe J. Erk5 activation inhibits inflammatory responses via peroxisome proliferator-activated receptor delta (ppardelta) stimulation. J Biol Chem. 2006; 281:32164–32174. [PubMed: 16943204]
25. Yan C, Luo H, Lee JD, Abe J, Berk BC. Molecular cloning of mouse erk5/bmk1 splice variants and characterization of erk5 functional domains. J Biol Chem. 2001; 276:10870–10878. [PubMed: 11139578]

26. Woo CH, Shishido T, McClain C, Lim JH, Li JD, Yang J, Yan C, Abe J. Extracellular signal-regulated kinase 5 sumoylation antagonizes shear stress-induced antiinflammatory response and endothelial nitric oxide synthase expression in endothelial cells. Circ Res. 2008; 102:538–545. [PubMed: 18218985]
27. Nigro P, Abe J, Woo CH, Satoh K, McClain C, O'Dell MR, Lee H, Lim JH, Li JD, Heo KS, Fujiwara K, Berk BC. Pkczeta decreases enos protein stability via inhibitory phosphorylation of erk5. Blood. 2010; 116:1971–1979. [PubMed: 20538799]
28. Pi X, Yan C, Berk BC. Big mitogen-activated protein kinase (bmk1)/erk5 protects endothelial cells from apoptosis. Circ Res. 2004; 94:362–369. [PubMed: 14670836]
29. English JM, Pearson G, Baer R, Cobb MH. Identification of substrates and regulators of the mitogen-activated protein kinase erk5 using chimeric protein kinases. J Biol Chem. 1998; 273:3854–3860. [PubMed: 9461566]
30. Iiyama K, Hajra L, Iiyama M, Li H, DiChiara M, Medoff BD, Cybulsky MI. Patterns of vascular cell adhesion molecule-1 and intercellular adhesion molecule-1 expression in rabbit and mouse atherosclerotic lesions and at sites predisposed to lesion formation. Circ Res. 1999; 85:199–207. [PubMed: 10417402]
31. Jongstra-Bilen J, Haidari M, Zhu SN, Chen M, Guha D, Cybulsky MI. Low-grade chronic inflammation in regions of the normal mouse arterial intima predisposed to atherosclerosis. J Exp Med. 2006; 203:2073–2083. [PubMed: 16894012]
32. Hilgarth RS, Murphy LA, Skaggs HS, Wilkerson DC, Xing H, Sarge KD. Regulation and function of sumo modification. J Biol Chem. 2004; 279:53899–53902. [PubMed: 15448161]
33. Itahana Y, Yeh ET, Zhang Y. Nucleocytoplasmic shuttling modulates activity and ubiquitination-dependent turnover of sumo-specific protease 2. Mol Cell Biol. 2006; 26:4675–4689. [PubMed: 16738331]
34. Lee MH, Mabb AM, Gill GB, Yeh ET, Miyamoto S. Nf-kappab induction of the sumo protease senp2: A negative feedback loop to attenuate cell survival response to genotoxic stress. Mol Cell. 2011; 43:180–191. [PubMed: 21777808]

Novelty and Significance

What Is Known?

- Disturbed flow in branches and bifurcations of the arterial tree promotes atherogenesis via endothelial cell apoptosis and inflammation.
- Sentrin/Small Ubiquitin-like Modifier (SUMO)-specific protease 2 (SENP2) catalyzes de-SUMOylation of proteins and thereby regulates localization, degradation, binding, and activity of SUMOylated proteins.
- Disturbed flow activates PKCζ-induced p53 SUMOylation and p53 binding to bcl2 in the cytoplasm, leading to EC apoptosis.
- SUMOylation of ERK5 inhibits laminar flow-induced expression of Kruppel-like factor 2 (KLF2), which is a key anti-inflammatory transcription factor, resulting in the loss of the anti-inflammatory effects of ERK5.

What New Information Does This Article Contribute?

- Both p53 and ERK5 were SUMOylated in response to disturbed, but not laminar, flow.
- Deletion of SENP2 enhanced disturbed flow-induced EC apoptosis and inflammation by up-regulating p53 and ERK5 SUMOylation, respectively.
- EC apoptosis, adhesion molecules expression, and atherogenesis were increased in both disturbed flow and steady laminar flow areas in Senp2+/− or Senp2+/−/Ldlr−/− mice aorta.
- The lesion size in the aortic arch of Senp2+/−/Ldlr−/− mice was much larger than that in descending aorta.

Several studies demonstrate that disturbed flow is pro-atherogenic. Here, we show that SENP2 plays a unique role in disturbed flow-induced EC apoptosis and inflammation via regulating p53 and ERK5 SUMOylation, respectively. We found that deletion of SENP2 enhanced disturbed flow-induced EC apoptosis and E-selectin and VCAM-1 expression, and subsequent atherosclerotic lesion formation. Notably, the lesion size in the aortic arch of Senp2 deficient mice, where ECs are mainly exposed by disturbed flow, was much larger than that in the descending aorta, suggesting the crucial role of SENP2 on atherogenesis under disturbed flow. Ldlr−/− mice that received Senp2+/− hematopoietic cells showed the same extent of atherosclerotic lesion formation as the mice given cells from Senp2+/− hematopoietic cells from Senp2+/+ donors, demonstrating the crucial role of vascular cell SENP2 on regulating atherogenesis. These findings reveal a novel pathway of SENP2-mediated SUMOylation of p53 and ERK5, which leads to EC dysfunction and increased atherogenesis especially under the disturbed flow.

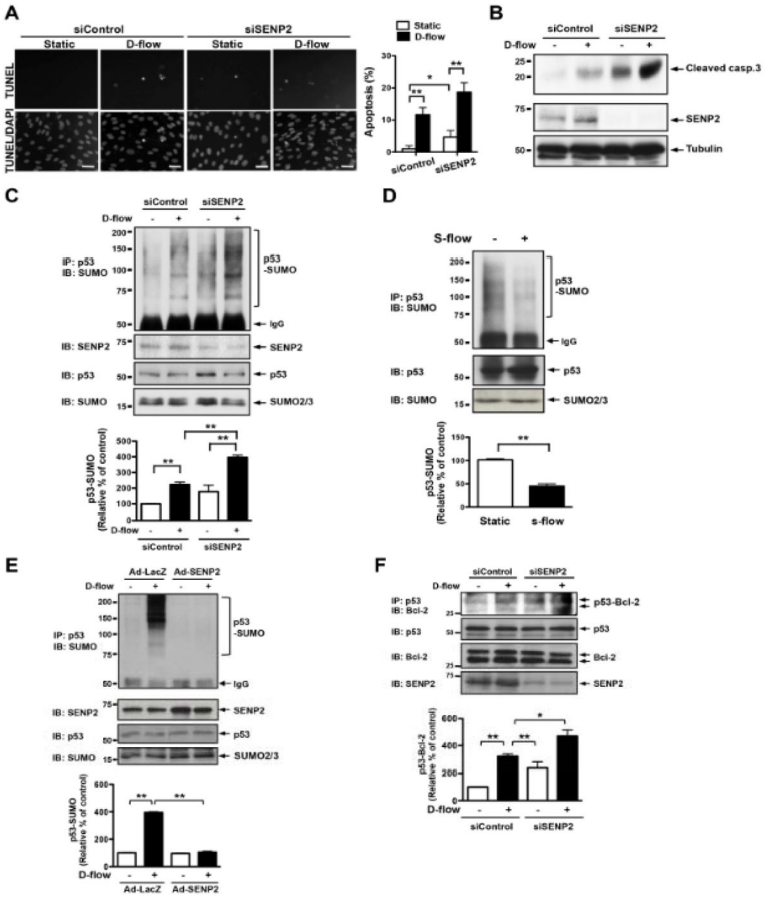

Figure 1. SENP2 inhibits endothelial apoptosis by regulating p53 SUMOylation

(A–B) HAECs were transfected with control or SENP2 siRNAs for 48 hrs and then stimulated by disturbed flow (d-flow) or no flow for 36 hrs. TUNEL staining (A) or Western blotting with anti-cleaved caspase3 antibody (B) was performed to determine apoptosis. (A) Images were recorded as described in Materials and Methods after counterstaining with DAPI to visualize nuclei (bottom). Apoptotic nuclei appear white and light-grey (top). Bars, 20μm. Quantification of apoptosis is shown as the percentage of TUNEL-positive cells (A, right panel). Shown is mean ± S.D., (n =3). ***P*<0.01, **P*<0.05. (B) Cleaved-caspase3 (casp. 3) expression was increased by transfection with SENP2 siRNA. SENP2 expression and protein loading were assessed by Western blotting with anti-SENP2 (middle) and anti-tubulin (bottom), respectively. Representative blots from duplicate experiments are shown. (C and E) HAECs (C) or HUVECs (E) were transfected with control or SENP2 siRNA for 48 hrs (C) or transduced with 50 MOI of Ad-LacZ or Ad-SENP2 for 16 hrs (E) and then stimulated by d-flow or no flow for 3 hrs. p53 SUMOylation was detected by immunoprecipitation with rabbit anti-p53 followed by Western blotting with mouse anti-SUMO2/3 (top). Expression of SENP2, p53, and SUMO is shown using antibodies against each of the respective proteins. p53 SUMOylation was quantified as described in Materials and Methods (bottom panel). Shown is mean ± S.D., (n =3), ***P*<0.01. (D) HUVECs were stimulated by steady laminar flow (s-flow) or no flow for 3 hrs. p53 SUMOylation was detected by immunoprecipitation with rabbit anti-p53 followed by Western blotting with mouse anti-SUMO2/3 (top). Expression of p53 and SUMO are shown using antibodies against each of the respective proteins. p53 SUMOylation was quantified as described in Materials and Methods (bottom panel). Shown is mean ± S.D., (n =3), ***P*<0.01. (F)

HUVECs were transfected with control or SENP2 siRNA for 48 hrs and stimulated by d-flow or no flow for 3 hrs. p53-Bcl-2 binding was detected by immunoprecipitation with rabbit anti-Bcl-2 followed by Western blotting with mouse anti-p53 (top). Expression of SENP2, p53, and Bcl-2 is shown using antibodies against each of the respective proteins. p53 and Bcl-2 binding was quantified as described in Materials and Methods (bottom panel). Shown is mean ± S.D., (n =3), $^{**}P<0.01$. D-flow, disturbed flow; Static, no flow; and S-flow, steady laminar flow.

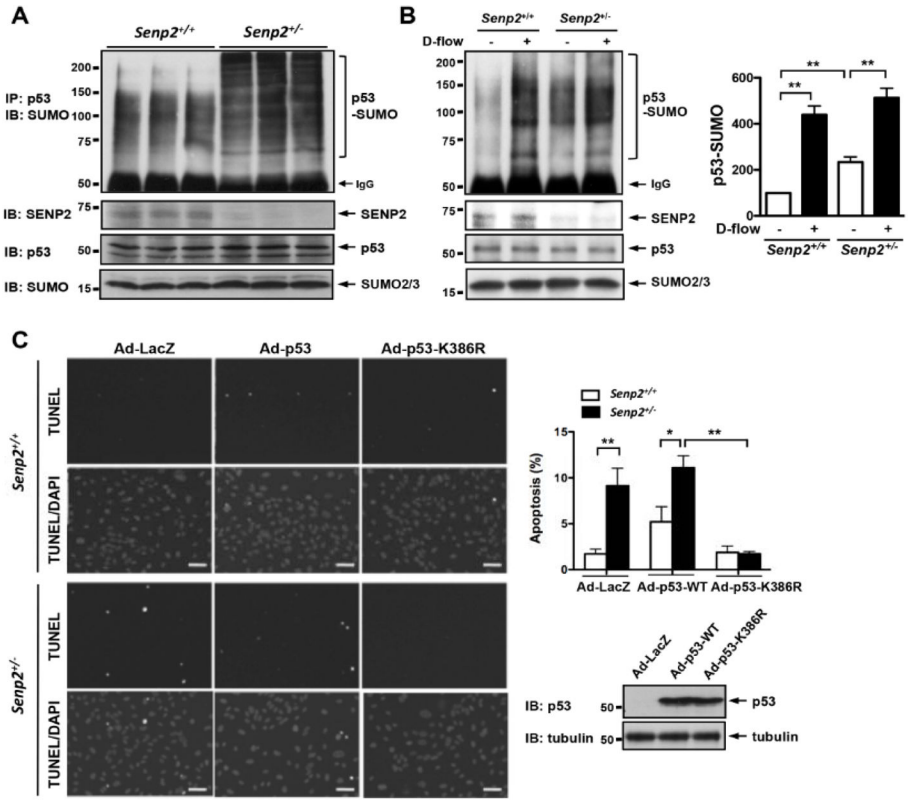

Figure 2. Reduced SENP2 expression increases p53 SUMOylation and apoptosis in mouse lung and aortic ECs

(A–B) p53 SUMOylation was studied with or without d-flow for 3 hrs in three different preparations of MLECs (A) or MAECs (B) isolated from *Senp2*$^{+/+}$ or *Senp2*$^{+/-}$ mice using immunoprecipitation with rabbit anti-p53 followed by Western blotting with mouse anti-SUMO2/3 (top). Antibodies specific to SENP2, p53, or SUMO2/3 were used to detect the expression level of each protein. p53 SUMOylation was quantified as described in Materials and Methods (bottom panel). Shown is mean± S.D., (n =3), ***P*<0.01. (C) MLECs isolated from *Senp2*$^{+/+}$ or *Senp2*$^{+/-}$ mice were transduced with indicated adenovirus (Ad) for 16 hrs and then analyzed for apoptosis by TUNEL staining. Cells were counterstained with DAPI (bottom). Apoptotic nuclei appear white and light-grey (top). Bars, 25μm. Quantification of apoptosis is shown as the percentage of TUNEL positive cells (C, right upper panel). **P*<0.05, ***P*<0.01. Expression levels of exogenous p53 and p53K386R were examined by Western blotting with anti-p53 (C, right lower panel).

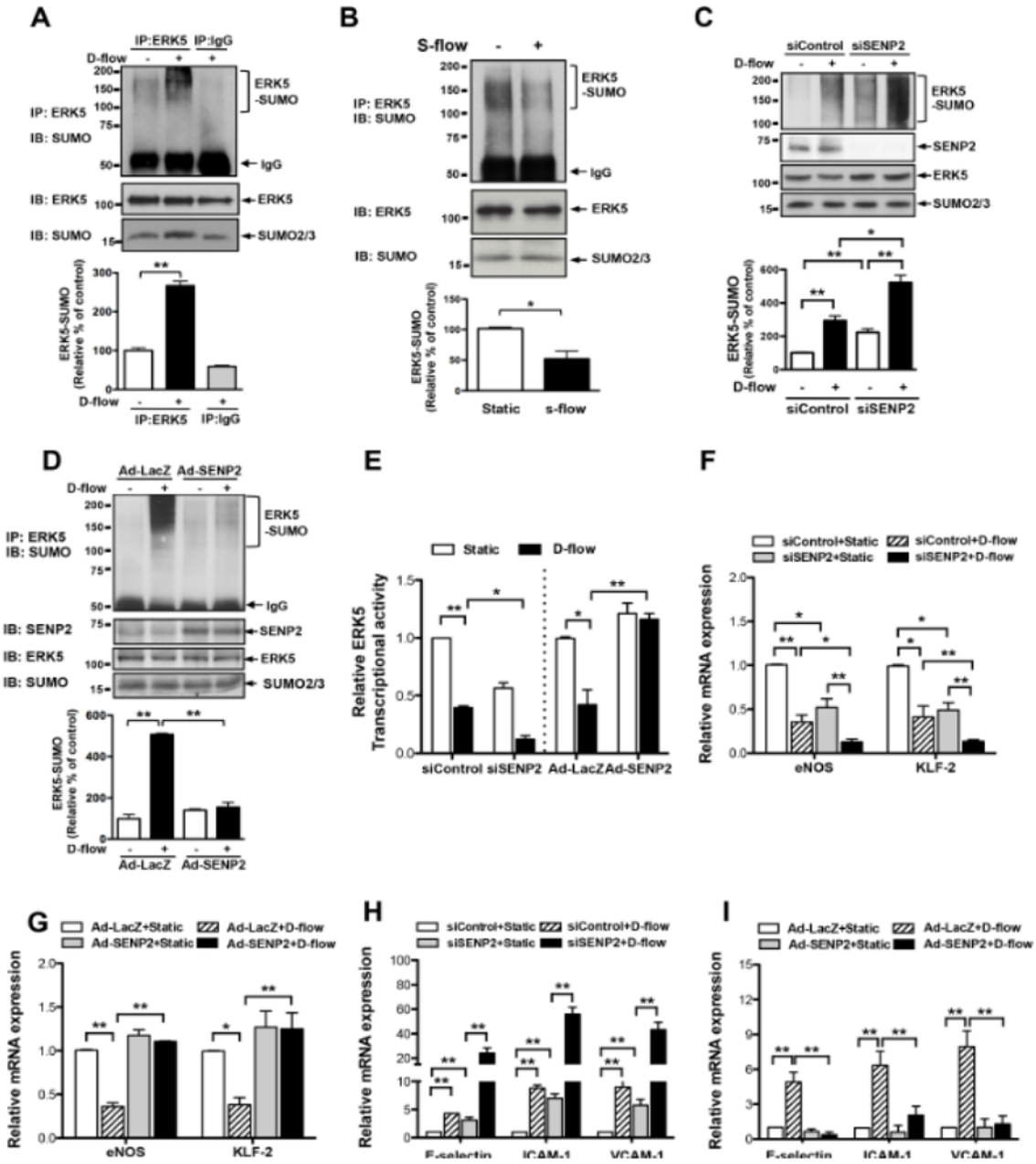

Figure 3. SENP2 inhibits disturbed flow-induced endothelial ERK5 SUMOylation

(A and B) HUVECs were stimulated by d-flow (A) or s-flow (B) for 3 hrs and their lysates were analyzed by immunoprecipitation with rabbit anti-ERK5 or IgG as a control. ERK5 SUMOylation was detected by Western blotting with mouse anti-SUMO2/3 (top). Expressions of ERK5 and SUMO were detected by using specific antibodies as indicated. p53 SUMOylation was quantified as described in Materials and Methods (bottom panel). Shown is mean ± S.D., (n =3). *P<0.05, **P<0.01. (C and D) HAECs (C) or HUVECs (D) were transfected with indicated siRNA for 48 hrs (C) or adenovirus for 16 hrs (D), and then stimulated by d-flow or no flow for 3 hrs. ERK5 SUMOylation was assessed as described in Fig. 3A. (E) HUVECs were transfected with SENP2 siRNA or control siRNA, or Ad-SENP2 or Ad-LacZ for 24 hrs and then transfected with Gal4-ERK5 and Gal4-responsive luciferase reporter pG5-*Luc*. After 18 hrs, cells were stimulated by d-flow or no flow for 6

hrs and then ERK5 transcriptional activity was assayed by a dual-luciferase reporter assay. Results were expressed as relative fold-changes vs. static cells in the siControl or LacZ control. Shown is mean ± S.D., (n =3). *P<0.05, **P<0.01. (F, G, H and I) HUVECs were transfected with SENP2 or control siRNA for 48 hrs or Ad-LacZ or Ad-SENP2 for 18 hrs followed by stimulation with d-flow or no flow for 24 hrs. Messenger RNA levels of E-selectin, ICAM-1, and VCAM-1 as inflammatory factors (F and G) and eNOS and KLF-2 as anti-inflammatory factors (H and I) were detected by qRT-PCR as described in methods. Results were expressed as relative fold-changes vs. static cells in the siControl or LacZ control. Shown is the mean ± S.D., (n =3). *P<0.05, **P<0.01.

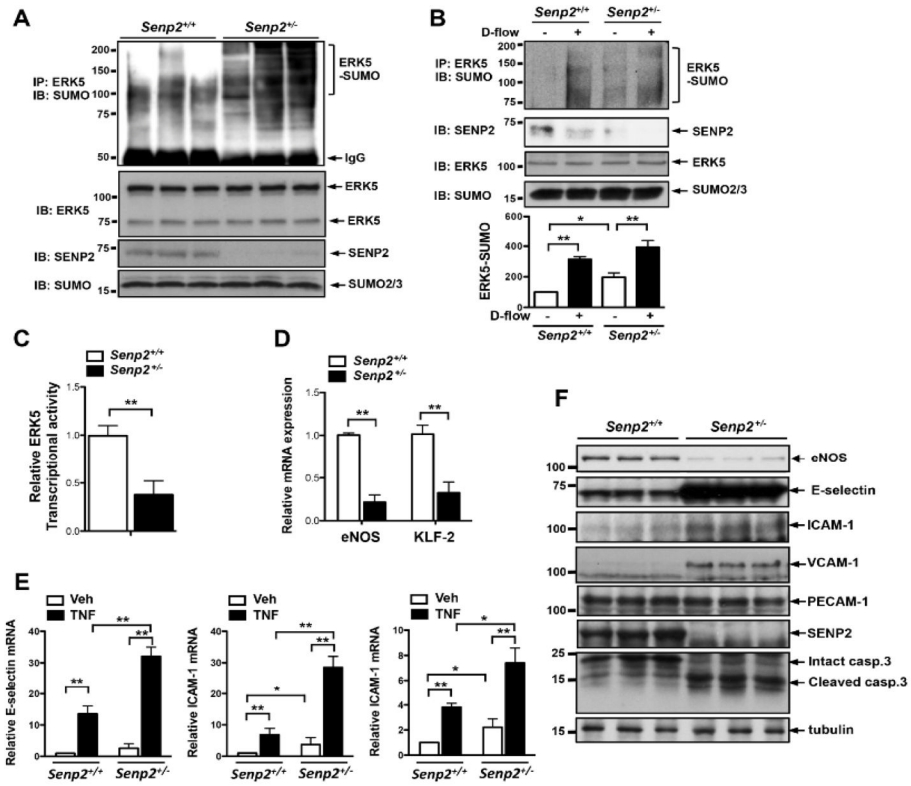

Figure 4. Disturbed flow inhibits ERK5 transcriptional activity and the expression of eNOS and KLF2 and increases adhesion molecule expression via SENP2

(A) ERK5 SUMOylation was studied in MLECs isolated from three different *Senp2*$^{+/+}$ or *Senp2*$^{+/-}$ mice using immunoprecipitation with rabbit anti-ERK5 followed by Western blotting with mouse anti-SUMO2/3 (top). SENP2, p53, or SUMO expression was detected by specific antibodies as indicated. (B) ERK5 SUMOylation was observed in MAECs isolated from *Senp2*$^{+/+}$ or *Senp2*$^{+/-}$ mice with or without d-flow for 3 hrs using immunoprecipitation with rabbit anti-p53 followed by Western blotting with mouse anti-SUMO2/3 (top). Antibodies specific to SENP2, p53, or SUMO2/3 were used to detect the expression level of each protein. p53 SUMOylation was quantified as described in Materials and Methods (bottom panel). Shown is mean± S.D., (n =3). **P*<0.05, ***P*<0.01. (C) ERK5 transcriptional activity was examined as described in Fig. 3E in MLECs from *Senp2*$^{+/+}$ and *Senp2*$^{+/-}$ mice. Shown is the mean ± S.D., (n =3). ***P*<0.01. (D) mRNA levels of eNOS and KLF-2 were determined by qRT-PCR as described in methods. Shown is the mean ± S.D., (n =3). ***P*<0.01. (E) mRNA levels of adhesion molecules in *Senp2*$^{+/+}$ or *Senp2*$^{+/-}$ MLECs treated with vehicle or TNFα for 6 hrs were assessed by qRT-PCR as described in the methods. Results were expressed as relative fold-increases vs. vehicle treated *Senp2*$^{+/+}$ cells. Shown is the mean ± S.D., (n =3). **P*<0.05, ***P*<0.01. (F) Expressions of eNOS, adhesion molecules as well as cleaved-caspase3 in MLECs isolated from three different *Senp2*$^{+/+}$ or *Senp2*$^{+/-}$ mice were determined by Western blotting. PECAM-1 expression was used to show the identity of cells as ECs. Veh, vehicle; and casp.3, caspase3.

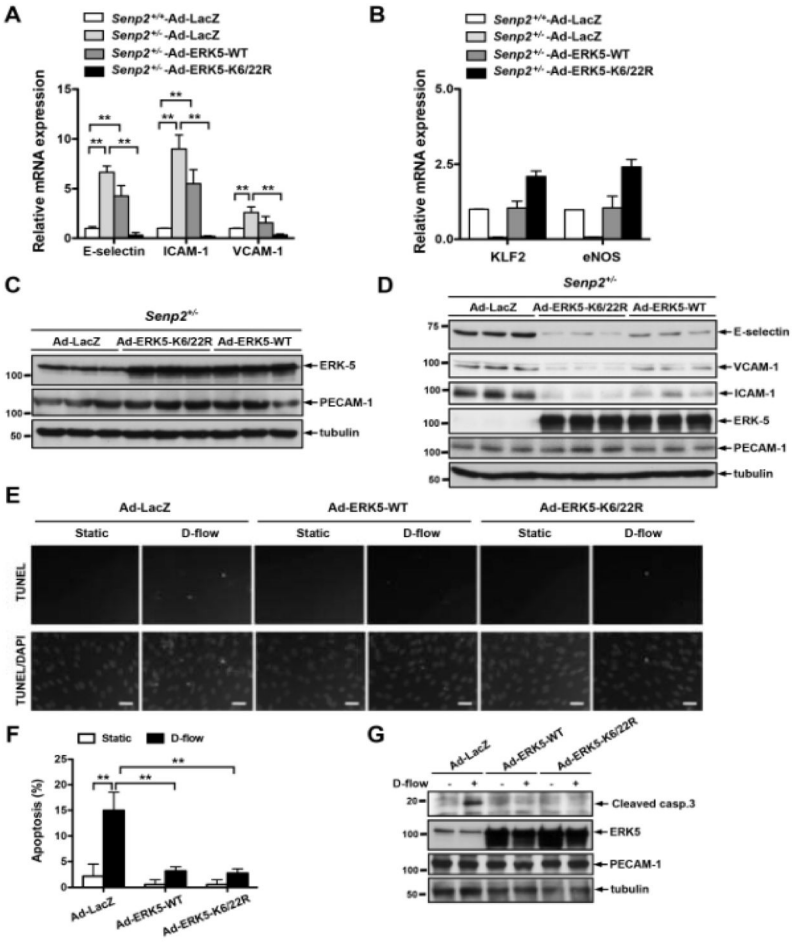

Figure 5. The crucial role of ERK5 SUMOylation in inflammation and apoptosis in MLECs and MAECs

(A, B) MLECs isolated from three different *Senp2*$^{+/-}$ mice were transduced with indicated Ad for 18 hrs and mRNA levels were determined by qRT-PCR using indicated specific primers as described in Fig. 3H. Shown is the mean ± S.D., (n =3). **P*<0.05, ***P*<0.01. (C) ERK5-WT and ERK5-K6/22R expression were confirmed by Western blotting. (D) MLECs isolated from three different *Senp2*$^{+/-}$ mice were transduced with indicated Ad for 18 hrs and expressions of adhesion molecules were determined by Western blotting with indicated antibodies. (E-G) MAECs from *Senp2*$^{+/+}$ mice were transduced with indicated Ad for 18 hrs and stimulated by d-flow for 36 hrs. TUNEL staining (E) or Western blotting with anti-cleaved-caspase3 (G) was performed. (E) Apoptotic and non-apoptotic nuclei appear white and light-grey (top) and grey (bottom), respectively. Bars, 20μm. (F) Quantification of apoptosis is shown as the percentage of TUNEL-positive cells. Shown is the mean ± S.D., (n =3). ***P*<0.01. (G) D-flow-induced cleaved-caspase3 expression was inhibited by Ad-ERK5-WT and Ad-ERK5-K6/22K transduction. ERK5 expression and protein loading were assessed by Western blotting with indicated antibodies. D-flow, disturbed flow; Static, no flow; and casp.3, caspase3.

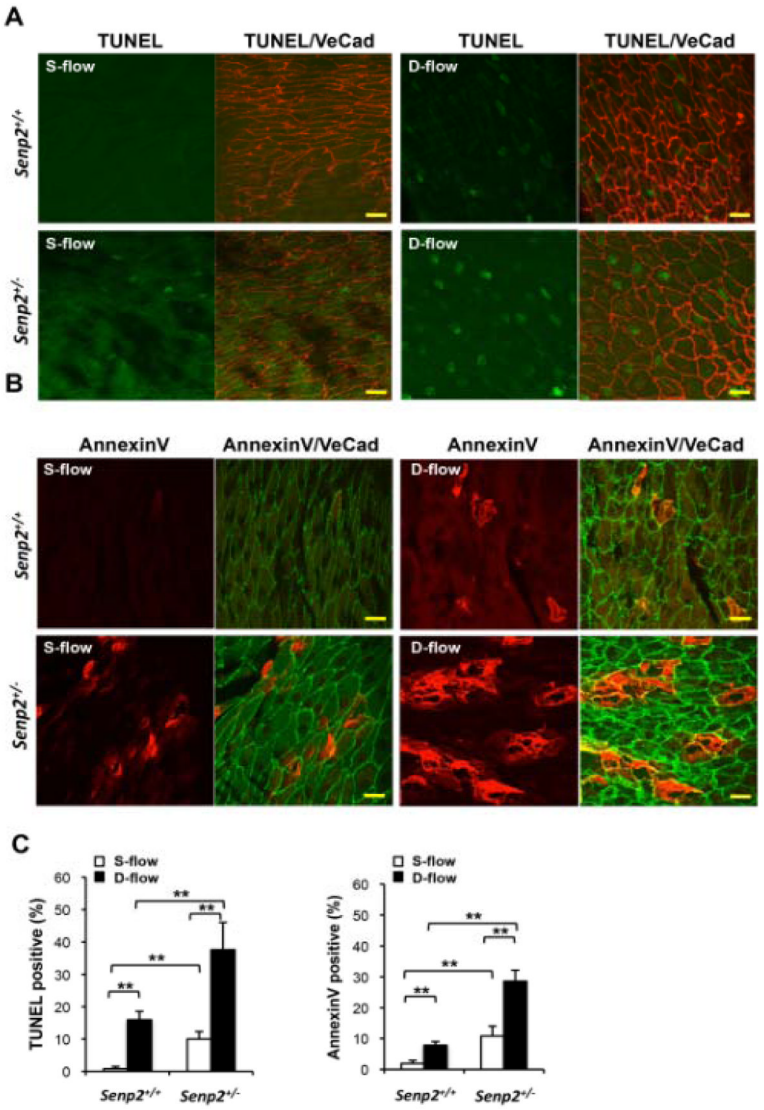

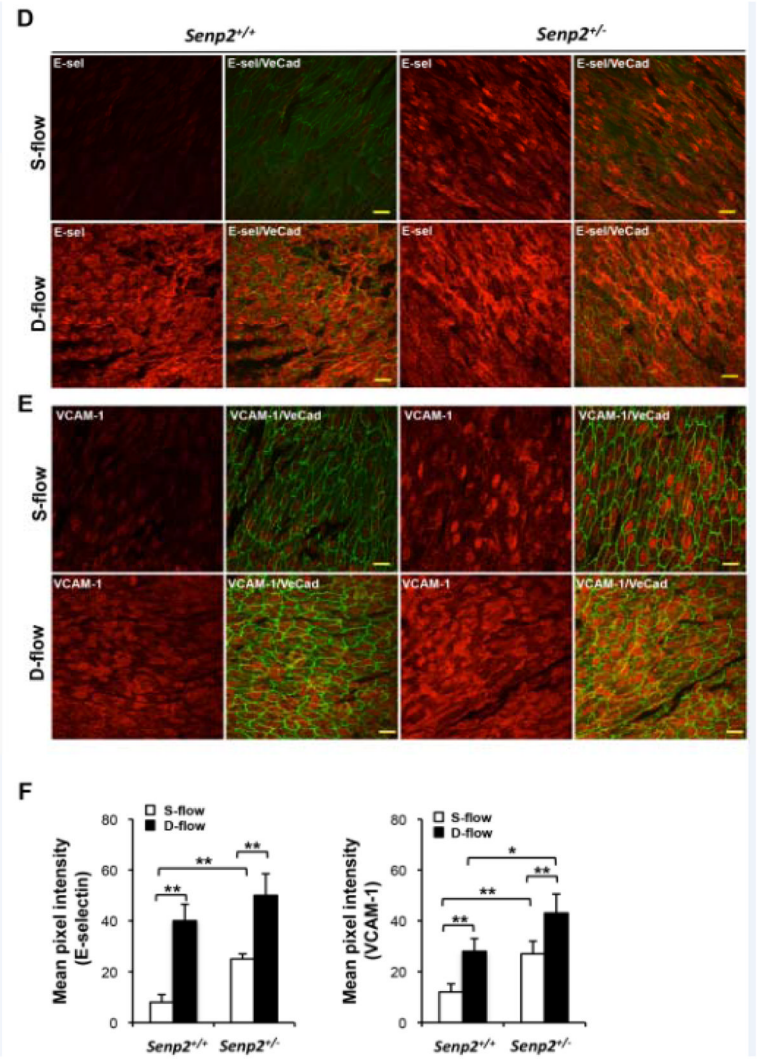

Figure 6. En face immunohistochemistry for EC apoptosis, E-selectin, and VCAM-1 in *Senp2*$^{+/+}$ and *Senp2*$^{+/-}$ mouse aorta

(A and B) EC apoptosis in the aortic arch of 7-week-old *Senp2*$^{+/+}$ or *Senp2*$^{+/-}$ mice. TUNEL- (green, A) or annexinV- (red, B) positive cells in both lesser (d-flow) and greater (s-flow) curvature areas were increased in the *Senp2*$^{+/-}$ compared with *Senp2*$^{+/+}$ mouse aorta. Anti-VE-cad staining was used as a EC marker. Bars, 20 μm. (C) Quantification of apoptotic cells examined by the TUNEL (left) or annexinV (right) assay (n=3 each). Data are shown as the mean ± S.D., ***P*<0.01. En face preparations were double-stained with anti-VE-cad and anti-E-selectin (D) or anti-VCAM-1 (E). A series of confocal optical section images were collected at a 0.5μm increment and a Z-stack image of about 4μm thickness from the luminal surface was obtained. From each image the background fluorescence intensity was subtracted and the pixel number of the stained region, per unit area, of the endothelium in d- and s-flow areas within the aortic arch from *Senp2*$^{+/+}$ or *Senp2*$^{+/-}$ mice were determined (n=3 each). Bars, 20μm. (F) Bar graphs show quantification of E-selectin (left) and VCAM-1 (right) in d- and s-flow areas of the aortic arch from *Senp2*$^{+/+}$ or *Senp2*$^{+/-}$ mice. Data are shown as the mean ± S.D., **P*<0.05, ***P*<0.01.

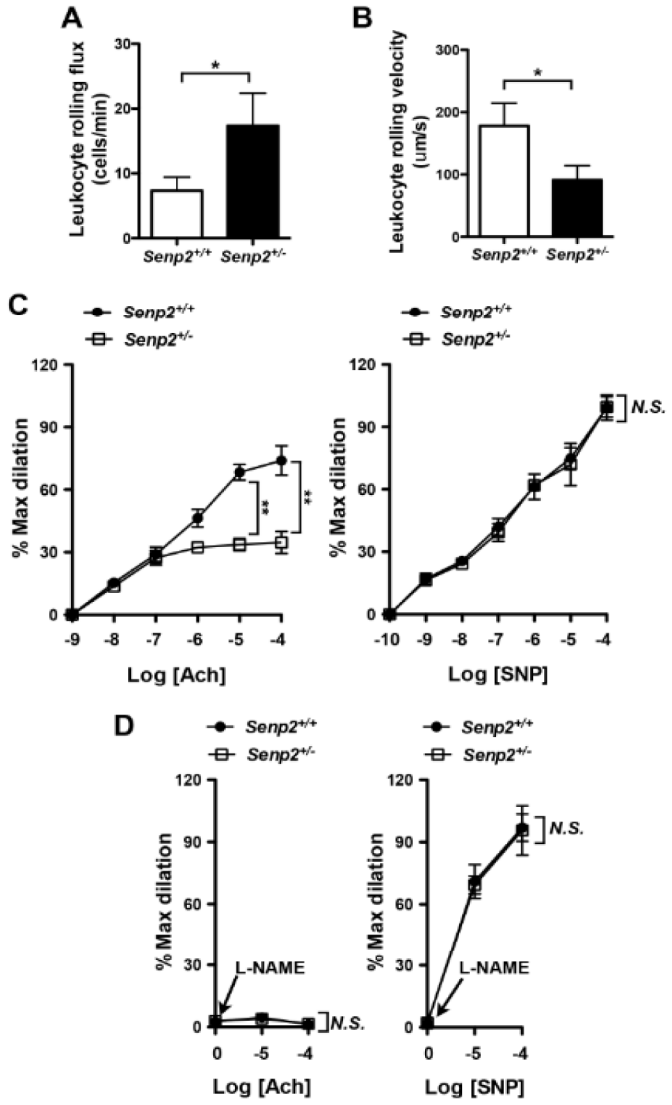

Figure 7. Increased leukocyte rolling and reduced endothelium-dependent vasodilatation in *Senp2*$^{+/-}$ mice

Leukocyte rolling *in vivo*. Quantified data on leukocyte rolling flux (A) and leukocyte rolling velocity (B) are shown. To analyze these parameters, image analysis software (NIS elements, Nikon) was used (n = 4, mean ± S.D.; **, P < 0.01). (C) Endothelium-dependent vessel relaxation by ACh (left) was inhibited, while SNP (right)-induced relaxation did not show any differences between *Senp2*$^{+/-}$ and *Senp2*$^{+/+}$ arterioles. At least, two arterioles per animals were examined. Data are shown as the mean ± S.D., n = 4 mice, ***P* < 0.01. (D) Effect of L-NAME on the ACh (left)- or SNP (right)-induced vessel dilation in arterioles of *Senp2*$^{+/+}$ and *Senp2*$^{+/-}$ mice. Data are shown as the mean ± S.D., n = 4 mice, ***P* < 0.01. Not significant, *N.S.*

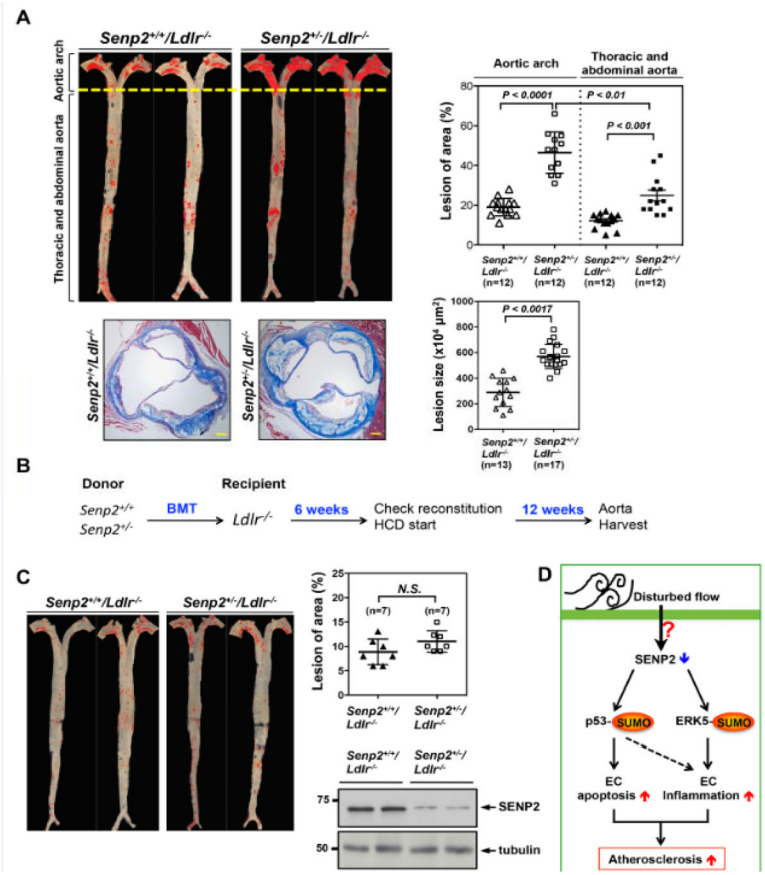

Figure 8. Reduced SENP2 expression accelerates atherosclerotic plaque formation, which is mediated by vascular but not by hematopoietic cells

Senp2$^{+/+}$/*Ldlr*$^{-/-}$ and *Senp2*$^{+/-}$/*Ldlr*$^{-/-}$ mice were given a high cholesterol diet for 16-week. *Senp2*$^{+/-}$/*Ldlr*$^{-/-}$ mice exhibited Oil red O-stained atherosclerotic lesions in the whole aorta, (top, left) as well as, increased Masson's trichrome stained atherosclerotic lesions in the cross-section of aortic valve region (bottom, left two). Bars, 50 μm. The graphs on the right show quantification of these data. Mean ± S.D. (n=12, whole aorta of *Senp2*$^{+/+}$/*Ldlr*$^{-/-}$ and *Senp2*$^{+/-}$/*Ldlr*$^{-/-}$; n=13, *Senp2*$^{+/+}$/*Ldlr*$^{-/-}$; and n=17, *Senp2*$^{+/-}$/*Ldlr*$^{-/-}$). The lesions of aortic arch compared to the lesion of descending aorta in the *Senp2*$^{+/-}$/*Ldlr*$^{-/-}$ mice are shown. ***P*<0.01. (B) The scheme of bone marrow transplantation. The transplantation of bone marrow cells from *Senp2*$^{+/+}$ or *Senp2*$^{+/-}$ mice into *Ldlr*$^{-/-}$ mice was performed and 6-week later, mice were given a high cholesterol diet for 12-week. (C) Atherosclerotic lesions were identified by Oil red O staining of the whole aorta (C, left). The graphs show quantified data (C, right upper). Mean ± S.D. (n=7). Not significant, *N.S.* The successful chimerism of BM cells was confirmed by Western blotting with anti-SENP2 using the blood cells after 6-weeks transplantation (C, right lower). (D) Schematic diagram showing the p53 and ERK5 SUMOylation signaling pathway mediating the EC apoptosis and inflammation to cause the atherosclerosis formation in response to disturbed flow.